Available online at www.sciencedirect.com
SCIENCE DIRECT®
Earth and Planetary Science Letters 243 (2006) 828–840
EPSL
www.elsevier.com/locate/epsl

Why dynamos are prone to reversals

F. Stefani *, G. Gerbeth, U. Günther, M. Xu

Forschungszentrum Rossendorf, P.O. Box 510119, D-01314 Dresden, Germany

Received 19 September 2005; received in revised form 6 January 2006; accepted 16 January 2006
Available online 3 March 2006
Editor: V. Courtillot

Abstract

In a recent paper [F. Stefani, G. Gerbeth. Asymmetric polarity reversals, bimodal field distribution, and coherence resonance in a spherically symmetric mean-field dynamo model. Phys. Rev. Lett. 94 (2005) 184506] it was shown that a simple mean-field dynamo model with a spherically symmetric helical turbulence parameter α can exhibit a number of features which are typical for Earth's magnetic field reversals. In particular, the model produces asymmetric reversals (with a slow decay of the dipole of one polarity and a fast recreation of the dipole with opposite polarity), a positive correlation of field strength and interval length, and a bimodal field distribution. All these features are attributable to the magnetic field dynamics in the vicinity of an exceptional point of the spectrum of the non-selfadjoint dynamo operator where two real eigenvalues coalesce and continue as a complex conjugated pair of eigenvalues. Usually, this exceptional point is associated with a nearby local maximum of the growth rate dependence on the magnetic Reynolds number. The negative slope of this curve between the local maximum and the exceptional point makes the system unstable and drives it to the exceptional point and beyond into the oscillatory branch where the sign change happens. A weakness of this reversal model is the apparent necessity to fine-tune the magnetic Reynolds number and/or the radial profile of α in order to adjust the operator spectrum in an appropriate way. In the present paper, it is shown that this fine-tuning is not necessary in the case of higher supercriticality of the dynamo. Numerical examples and physical arguments are compiled to show that, with increasing magnetic Reynolds number, there is strong tendency for the exceptional point and the associated local maximum to move close to the zero growth rate line where the indicated reversal scenario can be actualized. Although exemplified again by the spherically symmetric α^2 dynamo model, the main idea of this "self-tuning" mechanism of saturated dynamos into a reversal-prone state seems well transferable to other dynamos. As a consequence, reversing dynamos might be much more typical and may occur much more frequently in nature than what could be expected from a purely kinematic perspective.

Keywords: geomagnetic field; reversals; superchrons; superplumes

1. Introduction

The magnetic field of the Earth is known to undergo irregular reversals of its dipole part. The reversal rate is variable in the course of time: it was nearly zero in the Kiaman and the Cretaceous superchrons and is approximately 5 per My in the present [2].

Much effort has been devoted to identify typical characteristics of the reversal process. In particular, it was claimed that reversals may have an asymmetric, saw-toothed shape, with the field of one polarity decaying slowly and recreating rapidly with opposite polarity, possibly to quite high intensities [3–5].

* Corresponding author.
E-mail address: F.Stefani@fz-rossendorf.de (F. Stefani).

0012-821X/$ - see front matter © 2006 Elsevier B.V. All rights reserved.
doi:10.1016/j.epsl.2006.01.030

Another hypothesis concerns a correlation between the polarity interval length and the magnetic field intensity [6,7]. Associated with this, a causal connection of the Cretaceous superplume and superchron period has been discussed [8,9]. It was Vogt who first suggested a correlation between volcanism and reversal rate [10]. The general idea behind this is that superplumes give rise to an increased heat transport from the core mantle boundary to the Earth surface with the result of an increased dynamo strength due to a higher temperature gradient driving the outer core flow [11]. While this idea was soon generally accepted (with some counter-arguments regarding the involved time-scales [12]), quite contrary implications for the reversal frequency were drawn from it. The first "school", advocating a negative correlation of interval length and energy supply to the dynamo, goes back to Loper and McCartney [13]. The second school, suspecting long intervals for a strong dynamo, was motivated by various mean-field dynamo models, for which a transition from anharmonic oscillations to superchrons for increasing magnetic Reynolds number was observed [14].

A third, and still controversially discussed observation concerns the bimodal distribution of the Earth's virtual dipole moment (VDM) with two peaks at about 4×10^{22} A m^2 and at about twice that value [15–17].

For decades, it has been a challenge for dynamo theoreticians to explain reversals and their characteristics. It was considered a breakthrough when Glatzmaier and Roberts observed a reversal process in their fully coupled three-dimensional simulation of the geodynamo [18] (cf. also [19] for a recent overview). The strange thing with these simulations is that they reproduce many features of Earth magnetic fields, including reversals, quite well despite the fact that they are working in parameter regions far beyond those of the real Earth. This deficiency applies, in particular, to the Ekman and the magnetic Prandtl number. A way out of this dilemma may lie with a reliable sub-grid scale modeling [20]. In this respect one should also notice recent efforts to link direct numerical simulations and mean-field dynamo models [21,22].

This brings us back from expensive simulations to the complementary tradition of understanding reversals in terms of reduced dynamo models. A very simple approach in this direction is the celebrated Rikitake dynamo of two-coupled disk dynamos [23,24].

Another model was studied by Hoyng et al. [25–27]. A mean-field dynamo model is reduced to an equation system for the amplitudes of the non-periodic axisymmetric dipole mode and for one periodic overtone under the influence of stochastic forcing. This simple model, which produces sudden reversals and a Poissonian distribution of the interval time, has also been employed to simulate the phenomenon of stochastic resonance [28]. Stochastic resonance was made responsible in a former paper [29] for an apparent 100 ky periodicity in the interval length distribution [30] (note however, that this periodicity is not settled yet [31]). An essential ingredient of Hoyng's model to explain the correct reversal duration and the interval length consistently is the use of a large turbulent resistivity which is hardly justified. At least nothing of this has been seen in the recent liquid sodium dynamo experiments [32].

A further approach to understand reversals relies on the transition between non-oscillatory and oscillatory eigenmodes of the dynamo operator [33–35]. Those transition points, which have been found in many dynamo models [36,37], are well known in operator theory as spectral branch points—"exceptional points" of branching type of non-selfadjoint operators [38]. Such branch points are characterized not only by coalescing eigenvalues but also by a coalescence of two or more (geometric) eigenvectors and the formation of a non-diagonal Jordan block structure with associated vectors (algebraic eigenvectors) [39–41].[1] This is in contrast to "diabolical points" [45] which are exceptional points of an accidental crossing of two or more spectral branches with an unchanged diagonal block structure of the operator and without coalescing eigenvectors [38,40].

In a recent paper [1], we have analyzed the magnetic field dynamics in the vicinity of an exceptional point in more detail. Although the used model, a mean-field dynamo of the α^2 type with a supposed spherically symmetric helical turbulence parameter α, is certainly far beyond the reality of the Earth dynamo (owing, in particular, to the missing North–South-asymmetry of α) it exhibited all mentioned reversal features: asymmetry, a positive correlation of field strength and interval length, and bimodal field distribution.

All those features together were attributed to the very peculiar magnetic field dynamics in the vicinity

[1] We note that *selfadjoint* operators in Hilbert spaces (as they describe e.g. observables in closed quantum systems) have real spectra and a strictly diagonal spectral decomposition (a trivial Jordan block decomposition). Non-trivial Jordan block structures occur rather generically at spectral real-to-complex transition points of non-selfadjoint operators. Other physical systems (apart from the dynamo) described by non-selfadjoint operators with non-trivial Jordan block decompositions are, e.g., microwave resonators [42] as well as bianisotropic crystals and their optical singularities [43]. An extended discussion of the underlying mathematics can be found, e.g., in [44].

of an exceptional point. Usually, this exceptional point is associated with a local maximum of the growth rate curve at a slightly lower magnetic Reynolds number.

If this local maximum lies above zero, then there is a stable fixed point to the left of it. However, any prevailing noise can trigger the system to switch to the unstable fixed point at the right of the local maximum. From there the system is driven, in a self-accelerating way, to the exceptional point and beyond into the oscillatory branch where it undergoes the very polarity change and comes back to one of the fixed points.

If the local maximum is below zero, the system undergoes an anharmonic oscillation (a limit cycle) with a pronounced asymmetry of the "reversal". However, noise can lift the local maximum over zero making the system stay in the fixed point for a while before resuming the anharmonic oscillation.

This reversal scenario seems not unrealistic since it exhibits at least three reversal characteristics with only demanding the existence of an exceptional point and a nearby local maximum of the growth rate. The drawback is that it seems to require an artificial fine-tuning of the intensity and/or the spatial distribution of the dynamo source, in order to position the exceptional point and its accompanying local maximum close to the zero line. By checking a variety of α profiles in the *kinematic regime*, we have indeed observed that the spectral structure as it is necessary for reversals to happen occurs only seldom. Hence, the criticism that our particular choice of $\alpha(r)$ has not enough geophysical background to explain reversals [21] seems well justified.

Thus motivated, it is the main goal of the present paper to find better arguments why a dynamo operator should have a reversal-prone spectrum. A first hint on the solution of this puzzle can be found in the papers by Brandenburg et al. [46] and by Meinel and Brandenburg [47]. For a mean-field disc dynamo (which is rather a model for galactic than for planetary dynamos), it was shown [47] that a dynamo in *the highly supercritical regime* can exhibit a pronounced reversal behaviour, although this would not be expected from considering only the kinematic profiles of α.

In the present paper we will verify if this behaviour in the highly supercritical regime can be understood in terms of the "exceptional point model". Our main outcome will be that there is *a strong tendency of saturated dynamos to evolve into a reversal-prone state* where the condition, that the exceptional point and the local maximum are situated close to the zero line, is indeed fulfilled. Applied to the Earth, a possible conclusion could be that reversals are rather due to a *self-tuning* of the saturated geodynamo than to an accidental fine-tuning of its (hypothetical) kinematic pendant.

2. The model

Instead of simulating the real Earth dynamo with a fully coupled three-dimensional solver, we employ a very simple mean-field dynamo model in order to work out clearly the basic mechanism of reversals.

The considered α^2 dynamo with a spherically symmetric helical turbulence parameter α leads to a system of two coupled partial differential equations with only one spatial variable (the radius). This model is simple enough to allow for long-time simulations providing reasonable reversal statistics, but at the same time it is still complex enough to catch the essence of *hydro*magnetic dynamos. In contrast to their technical counterparts, the saturation of hydromagnetic dynamos relies strongly on the *deformability of the dynamo source* which is, in our case, the variable radial dependence of α. Note that in the quite different context of the Riga dynamo experiment a similar one-dimensional back-reaction model was used which reflects also the hydromagnetic character of this dynamo experiment in contrast to experiments with a more constraint geometric flexibility [48,49].

The magnetic field evolution of a kinematic α^2 dynamo is governed by the induction equation

$$\frac{\partial \boldsymbol{B}}{\partial \tau} = \nabla \times (\alpha \boldsymbol{B}) + \frac{1}{\mu_0 \sigma} \Delta \boldsymbol{B}, \tag{1}$$

with α denoting the helical turbulence parameter which may depend on the position $\boldsymbol{r}$ and the time τ [50]. The dynamo acts, within a sphere of radius R, in a fluid with electrical conductivity σ. The magnetic field has to be divergence-free, $\nabla \cdot \boldsymbol{B} = 0$. In what follows, the length will be measured in units of R, the time in units of $\mu_0 \sigma R^2$, and the parameter α in units of $(\mu_0 \sigma R^2)^{-1}$. Note that for the Earth we get a typical time scale $\mu_0 \sigma R^2 \sim 200$ ky, which results in a free decay time of 20 ky for the dipole field.

It is convenient to decompose $\boldsymbol{B}$ into a poloidal and a toroidal field component according to $\boldsymbol{B} = -\nabla \times (\boldsymbol{r} \times \nabla S) - \boldsymbol{r} \times \nabla T$. The defining scalars S and T are then expanded in spherical harmonics of degree l and order m with the expansion coefficients $s_{l,m}(r, \tau)$ and $t_{l,m}(r, \tau)$.

For the present case with $\alpha(\boldsymbol{r})=\alpha(r)$, the induction equation decouples for each l and m into the following pair of equations:

$$\frac{\partial s_l}{\partial \tau} = \frac{1}{r}\frac{\partial^2}{\partial r^2}(r s_l) - \frac{l(l+1)}{r^2} s_l + \alpha(r,\ \tau) t_l, \tag{2}$$

$$\frac{\partial t_l}{\partial \tau} = \frac{1}{r}\frac{\partial}{\partial r}\left[\frac{\partial}{\partial r}(r t_l) - \alpha(r,\tau)\frac{\partial}{\partial r}(r s_l)\right] - \frac{l(l+1)}{r^2}[t_l - \alpha(r,\ \tau) s_l]. \tag{3}$$

The boundary conditions are $\partial s_l/\partial r|_{r=1} + (l+1)s_l(1) = t_l(1) = 0$. In the following we focus our attention on the dipole mode with $l=1$, and will henceforth skip the corresponding subscript of s and t; $s := s_1$ and $t := t_1$. The absence of the order m in Eqs. (2) and (3) follows from the spherical symmetry of α. It implies, in particular, a complete degeneracy of axial and equatorial dipole modes. It is clear that for any more realistic model (e.g. with inclusion of the North–South asymmetry of α) this degeneracy would be lifted.

Let us assume that the profile of α in the kinematic regime, $\alpha_{\mathrm{kin}}(r)$, represents a supercritical dynamo. After self-excitation has occurred, magnetic field saturation is ensured by quenching the parameter α. We do this with the angularly averaged magnetic field energy which can be expressed in terms of $s(r,\ t)$and $t(r,\ t)$ [51]. This averaging over the angles, which represents a severe simplification, has been introduced in order to remain within the framework of the spherically symmetric α^2 model. In reality, of course, any quenching would introduce terms breaking the spherical symmetry of α.

In addition to the quenching effect, we assume the α-profile to be affected by "blobs" of noise which are considered constant within a correlation time τ_{corr}. Physically, this noise is not unnatural: it could be understood as a consequence of changing boundary conditions for the core flow, but also as a shorthand for the omitted influence of higher multipole modes on the dominant dipole mode.

Putting all together, $\alpha(r)$ takes on the time dependent form

$$\alpha(r,\ \tau) = C\frac{\alpha_{\mathrm{kin}}(r)}{1 + E_{\mathrm{mag}}(r,\ \tau)/E^0_{\mathrm{mag}}} + \Xi(r,\ \tau) \tag{4}$$

where E_{mag} is the magnetic energy, averaged over the angles,

$$E_{\mathrm{mag}}(r,\ \tau) = \frac{2s^2(r,\ \tau)}{r^2} + \frac{1}{r^2}\left(\frac{\partial(r s(r,\ \tau))}{\partial r}\right)^2 + t^2(r,\ \tau). \tag{5}$$

In the numerical scheme, the noise term $\Xi(r,\ \tau)$ will be treated in form of a Taylor expansion,

$$\Xi(r,\ \tau) = \xi_1(\tau) + \xi_2(\tau)\ r^2 + \xi_3(\tau)\ r^3 + \xi_4(\tau)\ r^4, \tag{6}$$

with the noise correlation given by $\langle \xi_i(\tau)\xi_j(\tau+\tau_1)\rangle = D^2(1-|\tau_1|/\tau_{\mathrm{corr}})\Theta(1-|\tau_1|/\tau_{\mathrm{corr}})\delta_{ij}$.

In summary, our model is governed by four parameters, the magnetic Reynolds number C, the noise amplitude D, a mean magnetic energy E^0_{mag} in the saturated regime, and the noise correlation time τ_{corr}.

The equation system (2)–(4) is time-stepped using an Adams-Bashforth method. For the following examples, the correlation time τ_{corr} has been set to 0.02, and E^0_{mag} has been chosen to be 100. The details of these choices are not very relevant. Roughly speaking, a shorter correlation time τ_{corr} would require a stronger noise amplitude D in order to yield the same effect.

3. Anharmonic oscillations in the vicinity of exceptional points

In [1] we had considered the following particular form of the kinematic α profile:

$$\alpha_{\mathrm{kin}}(r) = C(-21.5 + 426.4r^2 - 806.7r^3 + 392.3r^4). \tag{7}$$

Actually, this strange-looking Taylor expansion was the result of an Evolution Strategy search for oscillatory spherically symmetric α^2 dynamos [52]. For this $\alpha(r)$ profile, the growth rate dependence on C is shown as curve K_1 in Fig. 1b. "K" stands for kinematic, and the subscript "1" indicates the eigenfunction with the radial wavenumber 1. Correspondingly, K_2 denotes the eigenfunction with the radial wavenumber 2. K_1 and K_2 coalesce at the (leftmost) exceptional point E and continue as a pair of complex conjugate eigenvalues. At the upper exceptional point E′, the curves K_1 and K_2 split off again into a pair of real eigenvalues.

The critical value for this $\alpha(r)$ profile, $C=1$, lies on the oscillatory branch, enclosed between the two exceptional points E and E′. For slightly supercritical values of C, the time evolution is a nearly harmonic oscillation that becomes more and more anharmonic and asymmetric with increasing C.

At $C=1.2789$ this oscillation acquires nearly a rectangular form (Fig. 1a). For this extremely anharmonic oscillation we analyze, at the eight different instants 1...8 shown in Fig. 1a, the corresponding

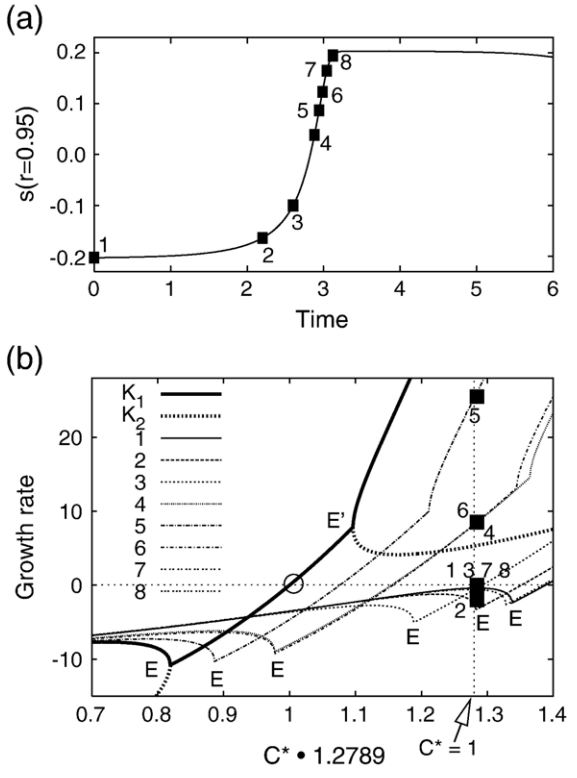

Fig. 1. (a) Part of an anharmonic oscillation showing the asymmetry of the reversals for the case $C=1.2789$. The points 1…8 indicate the instants which are analyzed in the text. (b) Growth rates for the kinematic profile (K) corresponding to Eq. (7) and for the quenched α profiles at the eight instants 1…8, in dependence on the artificial scaling factor C^*. The circle marks the critical point for the kinematic α profile. "E" indicates, for each of the considered α profiles, the lower exceptional point where the two first eigenmodes with radial wave numbers 1 and 2 coalesce. "E′" marks the second exceptional point, beyond which the two eigenvalues split and continue as real ones again.

instantaneous profiles $\alpha(r, \tau)$ (Fig. 2a). Governed by Eqs. (4) and (5), these instantaneous profiles depend on the instantaneous magnetic field variables $s(r, \tau)$ and $t(r, \tau)$, which are shown in Fig. 2b and c, respectively. For each of these instantaneous α profiles, the full squares on the vertical dashed line in Fig. 1b show the resulting instantaneous growth rate. In order to identify the position of these points with respect to the exceptional point, we scale the true quenched α profiles by an artificial factor C^*, according to $\alpha(r) = C^* \cdot 1.2789 \cdot (-21.5 + 426.4r^2 - 806.7r^3 + 392.3r^4)/(1 + E_{\mathrm{mag}}(r)/E^0_{\mathrm{mag}})$. Looking at the resulting lines 1…8 in the interval $0.7 < C^* \cdot 1.2789 < 1.4$ makes it possible to interpret a reversal in terms of the consecutive deformation of the original kinematic growth rate curve.

Let us begin with the instant 1. The magnetic field (Fig. 2b,c) is high, therefore the quenching of α is also quite strong (Fig. 2a). The resulting instantaneous growth rate (Fig. 1b) sits nearby the local maximum which is slightly below zero. Hence, the field starts to decay slowly.

At the instant 2, the field has already weakened, the quenching of α is less pronounced as before, and the point of the instantaneous growth rate has moved in between the local maximum and the exceptional point.

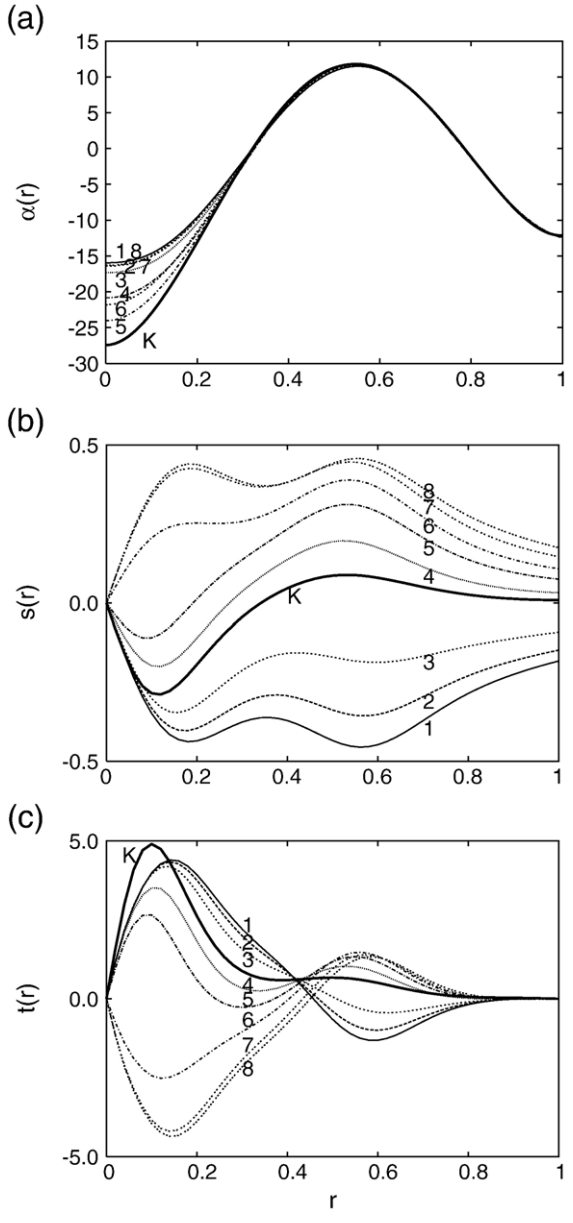

Fig. 2. Instantaneous α profiles and defining scalars of the magnetic field at the eight instants indicated in Fig 1a. (a) $\alpha(r)$. (b) $s(r)$. (c) $t(r)$.

At the instants 3 and 4, characterized by even weaker fields and less quenching of α, the growth rate point has reached the oscillatory branch. It follows a short intermezzo in the higher non-oscillatory branch (instant 5) where the α profile has nearly taken on the unquenched shape. After this, the system returns via the oscillatory branch (instant 6) to the reversed state at instants 7 and 8. It should be noted that this reversal scenario does not need any dramatic change or even a total sign reversal of α, as it was proposed e.g. in [53].

Readers familiar with the van der Pol oscillator [54] may notice that the signal form of Fig. 1a resembles strongly a "relaxation oscillation".[2] Indeed, a closer inspection of the dynamics of the van der Pol oscillator shows a similar behaviour of the leading instantaneous eigenvalues. To which extend the behaviour of the partial differential equation system (2)–(4) with r-dependent fields can really be reduced (by appropriate radial averaging) to that of the simple van der Pol equation, will be the subject of future considerations.

While for the considered value $C=1.2789$ the local maximum of the growth rate (points 1 and 8 in Fig. 1) was situated below zero, for larger C it will rise above the zero line. This way, we get two crossing points with the zero line. Since the crossing point at the left of the local maximum is a stable fixed point, we will get a steady field instead of the anharmonic oscillation considered so far. However, in the presence of noise this stable fixed point can be left and from time to time the system will undergo half an anharmonic oscillation. In this regime, the interval length is not anymore governed by the intrinsic frequency of the anharmonic oscillation, but by the intensity of the noise which triggers transition from the stable fixed point to the limit cycle considered above. For an illustration of this behaviour we refer the reader to Fig. 4 in [1].

4. Saturation into reversal-prone states

After the short review of [1] given in the last section, we are left with the impression that the indicated reversal scenario depends heavily on an artificial fine-tuning of the shape and the intensity of the $\alpha(r)$ profile.

In this section we will try to find better arguments for dynamos to be in a reversal-prone state. For this purpose, we change our focus from slightly supercritical dynamos to highly supercritical dynamos.

One comment is due in advance. The very particular α profile in Eq. (7) was the outcome of an Evolution Strategy search for an *oscillatory and dominant* dipole mode. In [52] it was shown that this double demand constrains the variety of possible $\alpha(r)$ profiles to a rather thin corridor. It is much easier to find profiles $\alpha(r)$ with an oscillatory $l=1$ mode for which some higher multipole modes with $l=2$, 3, … are dominant. In order not to overcomplicate the problem, in the following discussion we lift the demand for a dominant dipole mode by simply omitting any consideration of higher multiple modes.

Furthermore, instead of demanding from the onset the *kinematic* dynamo to be oscillatory, we will examine various simple analytical α profiles with respect to the resulting steady or oscillatory field behaviour, with special focus on the saturated states in the strongly supercritical regime.

Let us start with the classical profile $\alpha_{\rm kin}(r)=C$ which is known to possess only real eigenvalues for all C [50]. For the sake of concreteness, we consider the critical value $C=4.49$ and the supercritical values $C=10$, 20, and 50. We solve the induction equation systems (2) and (3) coupled to the quenching Eqs. (4) and (5). The quenched α profiles, $\alpha(r)=C/(1+E_{\rm mag}(r)/E^0_{\rm mag})$, which are shown in Fig. 3b, are then multiplied by a scaling parameter C^*, and the resulting instantaneous growth rate curves in dependence on C^* are shown in Fig. 3a. As in the former section, this procedure is intended to identify the position of the actual growth rate point with respect to the exceptional point.

Fig. 3b shows that the quenching of α is not homogenous along the radius. The saturation mechanism modifies the original constant α in such a way that there is a stronger suppression for smaller radii (evidently, because the magnetic field is strongest in the central part of the dynamo). This modification of the *shape* of α has a remarkable consequence for the spectrum. In Fig. 3a we see that the growth rate curves acquire an exceptional point which is moving toward the zero growth rate line with increasing C. In this particular example, the exceptional point does not drop below zero. Nevertheless, we will find later (Fig. 9a) that even in this case the noise can trigger reversals.

The next example, $\alpha_{\rm kin}=5/3Cr^2$, is illustrated in Fig. 4 (the factor 5/3 results from normalizing the radial average of $\alpha(r)$ to the value for constant α). The general tendency is the same as for the previous example $\alpha_{\rm kin}=C$, but now the exceptional point drops clearly below the zero line, leaving the maximum of this curve only slightly above zero. For $C=50$, say, the dynamo will "sit" on the stable fixed point at the left of the local maximum. At this point the field is rather strong. However, any noise can trigger a move to the unstable

[2] We thank Clement Narteau for drawing our attention to this point.

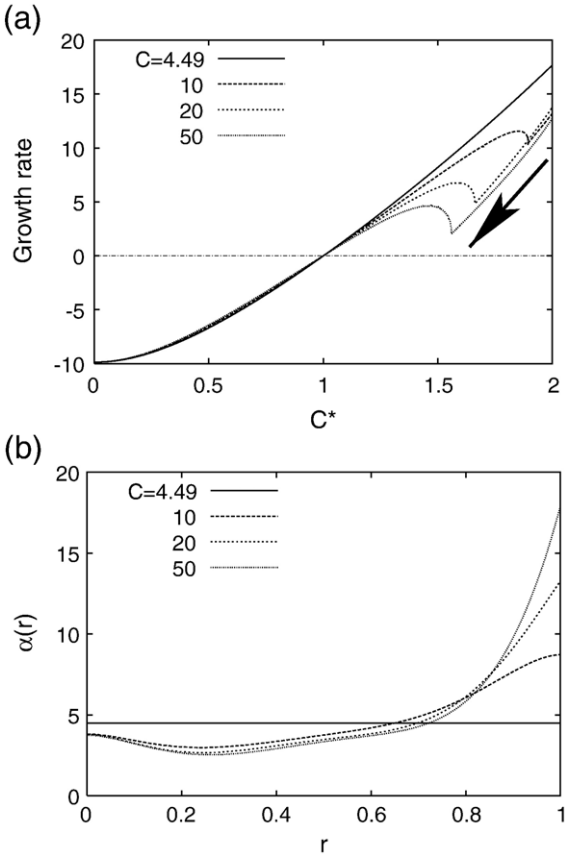

Fig. 3. (a) Growth rates for the profiles $\alpha(r)=C^*\cdot C/(1+E_{\rm mag}(r)/E^0_{\rm mag})$ with $C=10$, 20, 50. The quenched states, that correspond (for all chosen values of C) to $C^*=1$, are situated in all cases on the non-oscillatory branch. (b) Kinematic and quenched profiles $\alpha(r)$ for the four considered values of C.

fixed point at the right of the local maximum from where the reversal process can start.

The next example is $\alpha_{\rm kin}=6/3Cr^3$. Here the local maximum drops below the zero line for $C=20$ and 50 (Fig. 5). That means there is no stable fixed point anymore, the system runs into a limit cycle in form of the previously analyzed anharmonic oscillation. Therefore, α is changing its shape during this process. The curves "20 (m)" and "50 (m)" refer to those α profiles which are maximally quenched during the oscillation.

The last example, $\alpha_{\rm kin}(r)=5.75/3C(1-6r^2+5r^4)$, is quite similar to the example from [1], but it will provide a surprise (Fig. 6). Starting from the kinematic α, for which the exceptional point is well below the zero line, it rises rapidly above zero to a maximum value, but for even higher C it moves back in direction of the zero line. Evidently, there are two different mechanisms at work here.

All four considered examples exhibit a tendency for supercritical dynamos to saturate in a state for which the exceptional point and its associated local maximum lie close to the zero growth rate line. Interestingly enough, this happens independently on whether the exceptional point in the kinematic case was above the zero line (including the limiting case that there was no exceptional point at all) or below it.

What is the physical rationale behind this phenomenon? Back-reaction for hydromagnetic dynamos is quite generally an actualization of Lenz's rule stating that the excited magnetic field acts against the source of its own generation. For the considered model this means that the α profile is deformed in such a way that the growth rate is decreasing. For the example $\alpha_{\rm kin}=5/3Cr^2$, this effect is illustrated in Fig. 7a. We consider two cases: the marginal value $C=6.88$ and the slightly supercritical value $C=8.0$. In contrast to Figs. 3–6, the abscissa is now the quantity C^*C. This illustrates better how the first and the second radial eigenvalue curves are bent down. As a result, the back-reaction has a tendency

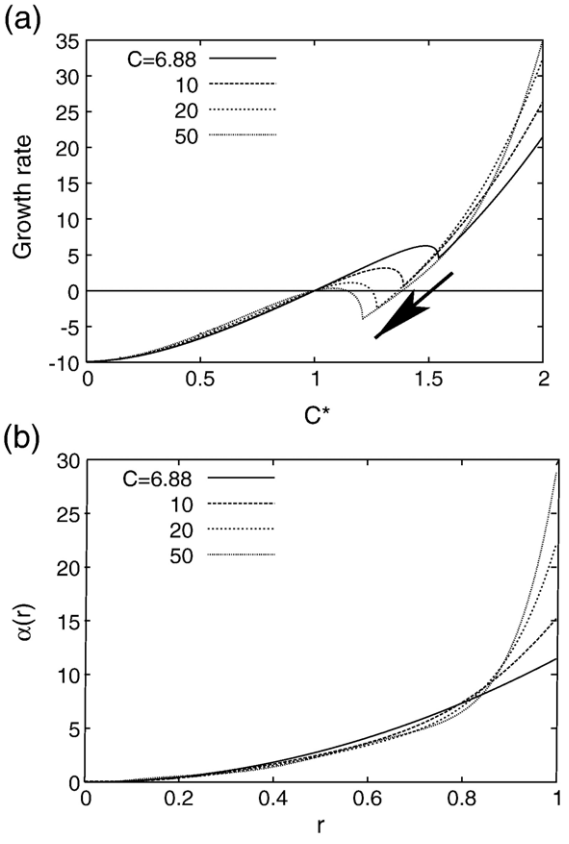

Fig. 4. Same as Fig. 3, but for $\alpha(r)=5/3C^*\cdot Cr^2/(1+E_{\rm mag}(r)/E^0_{\rm mag})$, for which the critical value is $C=6.88$.

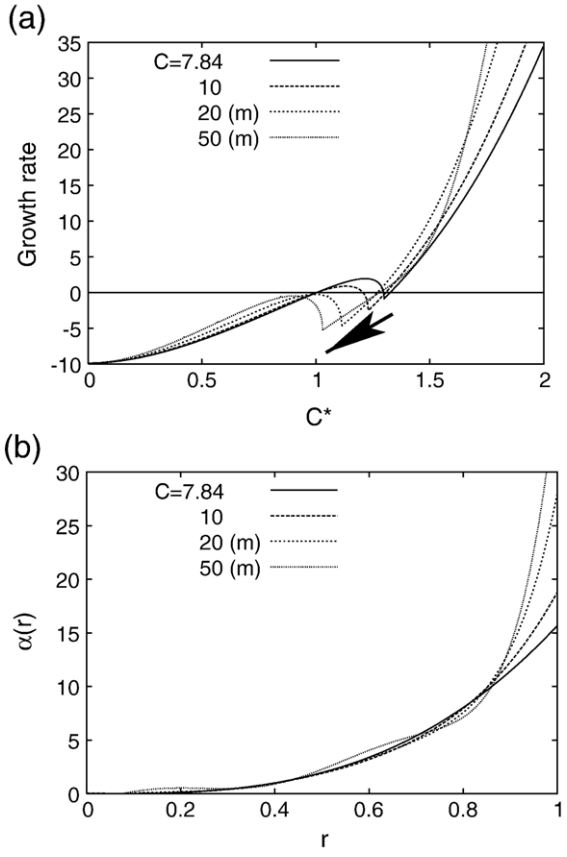

Fig. 5. Same as Fig. 3, but for $\alpha(r)=6/3C^*\cdot Cr^3/(1+E_{\mathrm{mag}}(r)/E^0_{\mathrm{mag}})$ for which the critical value is $C=7.84$. The labels "20 (m)" and "50 (m)" refer to the maximally quenched α profiles during the anharmonic oscillation.

to move the exceptional point downward in direction of the zero line (Fig. 7a).

While this argument is rather intuitive for the first three examples, it does not apply to the fourth example $\alpha_{\mathrm{kin}}(r)=5.75/3C(1-6r^2+5r^4)$ in which an exceptional point is already existent below the zero line. Again, back-reaction is expected to lower the growth rate, but now the most efficient way to do this is quite different. Fig. 7b may help to illustrate the essential point by depicting the growth rate curves for the marginal value $C=6.78$ and for $C=8$. For $C=6.78$, the eigenvalues with radial wave numbers $n=1$ and $n=2$ have already coalesced and formed an oscillatory eigenmode below the zero line. Now, since this oscillatory branch is very steep, the most efficient way of back-reaction is to return to the much flatter real branch. This means, in turn, that the local maximum and the exceptional point are even risen beyond the zero line. Only later, when the exceptional point is already well above the zero line, any further increase of C will promote the previous saturation mechanism, driving the exceptional point again back to the zero line (cf. Fig. 6). Comparing the length of the arrows in Fig. 7a and b, we see indeed that the growth rate reduction (i.e. the efficiency of back-reaction) is more pronounced by the second mechanism.

At present, work is in progress to support this rather intuitive and numerically derived picture by a paradigmatic analytical model.

In some respect, this self-tuning mechanism is similar to the concept of *self-organized criticality* [55], although it seems too early to over-stress this resemblance.

5. Time series and reversal duration

The time evolution of the considered dynamos is, in the noise-free case, determined by the position of the local maximum of the growth rate curve relative to the

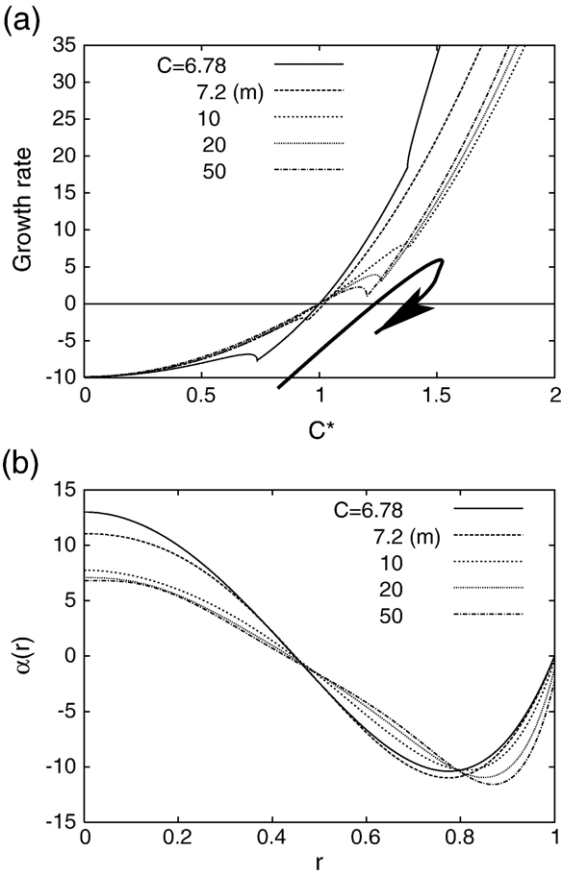

Fig. 6. Same as Fig. 5, but for $\alpha(r)=5.75/3C^*\cdot C(1-6r^2+5r^4)/(1+E_{\mathrm{mag}}(r)/E^0_{\mathrm{mag}})$ for which the critical value is $C=6.78$, leading to an oscillatory mode. The label "7.2 (m)" indicates again the maximally quenched α. Note the move of the exceptional point well above the zero line and back to it.

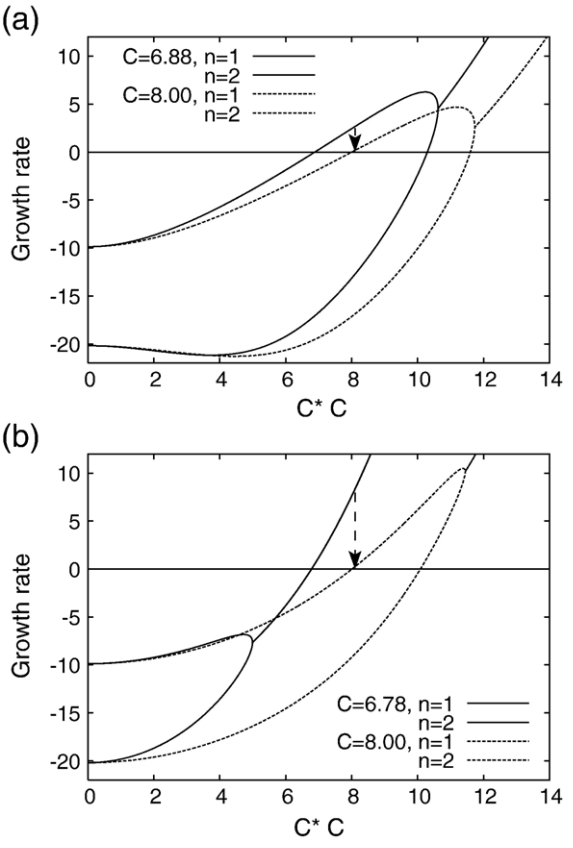

Fig. 7. The self-tuning mechanism of reversing dynamos. (a) Case that the exceptional point is above zero in the kinematic regime. Example $\alpha(r)=5/3C^*\cdot Cr^2/(1+E_{\rm mag}(r)/E^0_{\rm mag})$, with $C=6.88$ (critical value) and $C=8.0$. (b) Case that the exceptional point is below zero in the kinematic regime. Example $\alpha(r)=5.75/3C^*\cdot C(1-6r^2+5r^4)/(1+E_{\rm mag}(r)/E^0_{\rm mag})$ with $C=6.78$ (critical value) and $C=8.0$.

zero line. If the local maximum is below zero, than we get a limit cycle in form of an anharmonic oscillation, the mechanism of which has been described in detail above and in [1]. If the local maximum is situated well above the zero line, then the system runs into a stable fixed point. In case that the maximum is only slightly above zero, then a hysteretic behaviour may occur, in which the choice of the stable fixed point or the limit cycle is controlled by the strength of the pre-existing magnetic field.

A quantity which is of particular geophysical relevance is the duration of a reversal. Here is not the place to discuss the variety of different definitions, and all questions concerning the dependence of the apparent reversal duration on the site latitude [56]. Since our model relies exclusively on the evolution of the dipole field, we cannot use any definitions based on directional changes. For that reason we had employed in [1] a "working definition" of a reversal duration, based on the period during which the modulus of the magnetic field is smaller than a certain percentage of the amplitude of the (anharmonic) oscillation. For a value of 25% (which was motivated by demanding the dipole field to decay until this value in order that the non-dipole field can become dominant) we obtained a reversal duration of $0.15\tau_{\rm diff}$. For an assumed diffusion time of 200 ky, this would amount to 30 ky.

Now we would like to know how this reversal duration changes with increasing magnetic Reynolds number, in particular for highly supercritical dynamos. In Fig. 8 we plot the details of the reversal process for the third example of the previous section, $\alpha_{\rm kin}(r)=6/3Cr^3$. For C we have chosen the four values 20, 50, 100, and 200. Whatever the exact definition of a reversal might be, the tendency is clear: with increasing C, the reversal duration decreases significantly. This has to do with the fact that during the reversal the magnetic field gets weak and the α profile comes close to its unquenched, kinematic shape for which extremely high instantaneous growth rates and frequencies (only in the oscillatory branch) occur. These are responsible for a very fast reversal process. If we would define the reversal duration as the period during which the field is between ±50% of the oscillation amplitude, we would get for $C=200$ a time span of $0.03\tau_{\rm diff}$, corresponding to 6 ky. The corresponding time for $C=20$ is $0.09\tau_{\rm diff}$, i.e. 18 ky. Evidently, we can get a realistic time scale without taking resort to turbulent resistivity, as it was done in other reversal models [25].

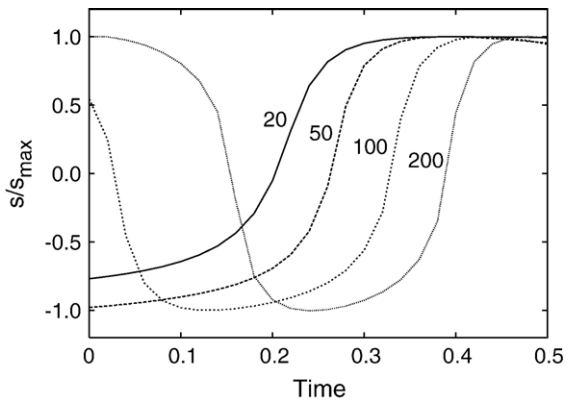

Fig. 8. Details of the reversal process for $\alpha_{\rm kin}=6/3Cr^3$ with the particular values $C=20$, 50, 100, and 200. The time scale is the diffusion time, which is approximately 200 ky for the Earth. Evidently, the reversal duration decreases significantly with increasing C and reaches values of ~10 ky for large C.

So far, we have considered the noise-free case. As already remarked, the role of noise depends on the position of the local maximum of the growth rate curve relative to the zero line. If it is above zero, the dynamo is usually at the fixed point characterized by a strong magnetic field, then the noise can trigger transitions to the unstable fixed point at the right of the local maximum, from where a reversal process can start. However, although being unstable, this fixed point can hold the system for a while (since the growth rate is zero there) making a second peak in the field strength histogram possible [1]. If the local maximum is below zero, making the dynamo undergo anharmonic oscillations with a weak field amplitude, then the noise can make it jump time by time to the strong field state.

Anyway, the noise will soften the differences between the two regimes with the local maximum below or above zero. In either case, there will be noise-strength dependent exchange between the fixed point state with a strong field and the limit cycle with a weak field.

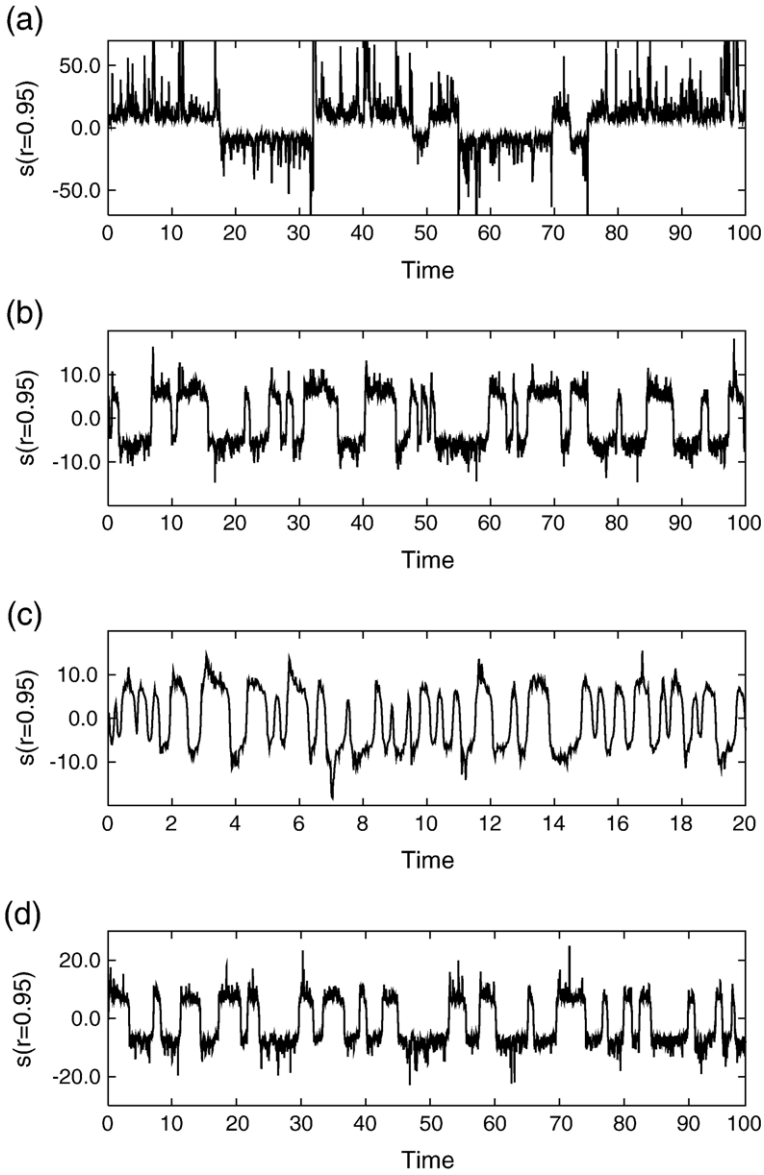

Fig. 9. Typical time series for the inclusion of noise. (a) $\alpha_{kin}(r)=C$. (b) $\alpha_{kin}(r)=5/3Cr^2$. (c) $\alpha_{kin}(r)=6/3Cr^3$. (d) $\alpha_{kin}(r)=5.75/3C(1-6r^2+5r^4)$. In all cases, we have chosen $C=50$. In the case (a), we have set $D=7$, in all other cases (b–d) $D=4$.

In Figs. 9 and 10 this is illustrated by some typical time series for the four dynamo examples considered in the previous section. In all cases we have chosen $C=50$. The noise intensity, D has been set to 4, apart from the first example with $\alpha_{\mathrm{kin}}=C$ for which a value of $D=7$ has been chosen to provoke any reversal at all.

Apart from details concerning the mean reversal rate and the transient excursions to rather high values, all the signals share the property that there are long time intervals without reversals and rather fast reversal processes.

A last remark concerns the long-standing problem of positive or negative correlation of energy supply and interval length. Our model is not able to solve this problem, but it can illustrate its intricacy. The first point is that any additional energy supply will increase both the magnetic Reynolds number C and the noise level D. Even if considered separately from D, the influence of C depends on whether it will lift or lower the local maximum with respect to the zero line. We have seen that both can happen, but for high supercriticality there is a general tendency of lowering the local maximum.

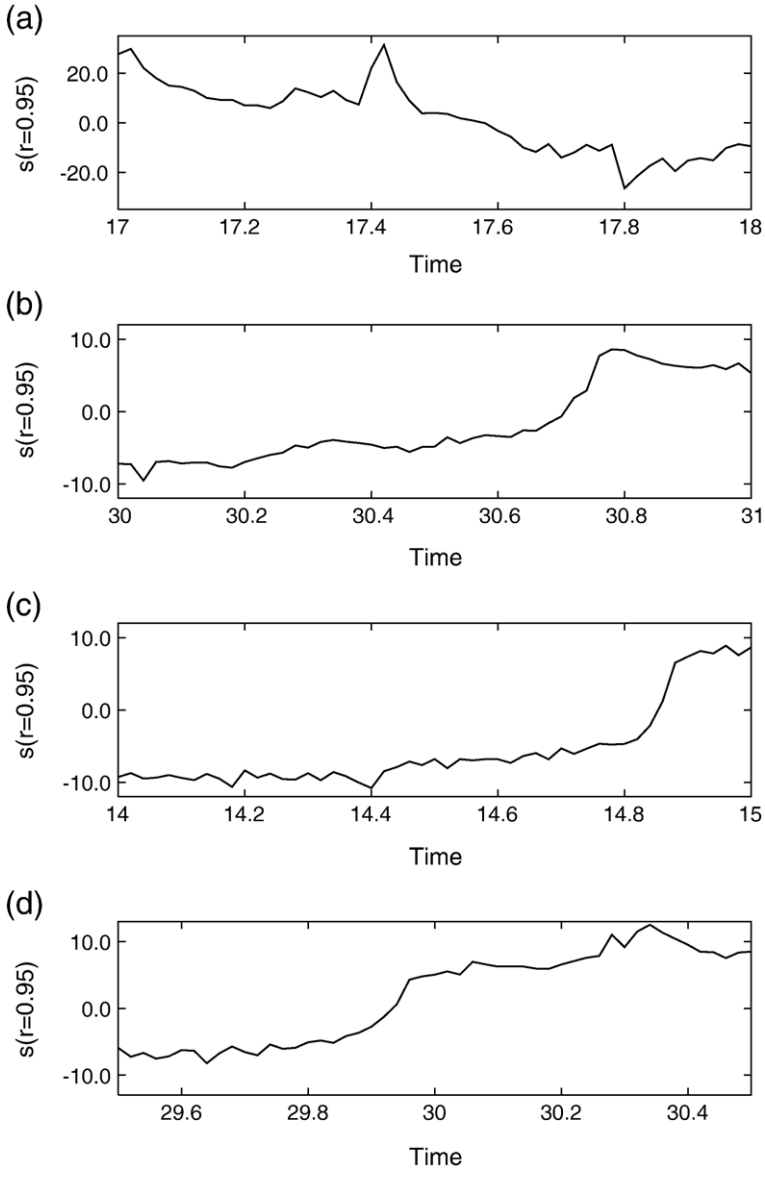

Fig. 10. Same as Fig. 9, but zoomed into time periods were one reversal occurs.

This would imply a negative correlation of energy supply and interval length, as it is also visible in Fig. 8. If considering the influence of D separately from C, we get also a complicated behaviour with a tendency toward a negative correlation of D and the interval length, but with a positive correlation for the case that the local maximum is below zero and the noise is weak (cf. Fig. 7 of [1]). Taken all together we get a very complex picture with no definite answer.

6. Conclusions

In [1] we had analyzed a reversal scenario that relies heavily on the existence of an exceptional point of the non-selfadjoint dynamo operator. We had shown that reversals can (a) be asymmetric, (b) yield a positive correlation of dynamo strength and interval length, and (c) show a pronounced bimodal field distribution. All three features have been recently discussed as being typical for reversals of the Earth's magnetic field.

The apparent weakness of this model, the necessity of fine-tuning the spatial structure of the dynamo source in order to bring the exceptional point and its associated local growth rate maximum close to the zero line, has been overcome in the present paper. We have shown that the back-reaction of the magnetic field has a strong tendency to drive the dynamo into a state where the indicated spectral conditions for reversals are indeed fulfilled.

This shows that dynamos with a high, but not necessarily extreme, supercritical magnetic Reynolds number are very prone to reversals. Hence, the proposed reversal scenario which might look contrived and hardly realistic from a purely kinematic point of view, becomes rather natural when seen from the side of the saturation process. The artificial fine-tuning for the regime of slightly supercritical dynamos is replaced by a self-tuning saturation into reversal prone states when it comes to highly supercritical dynamos.

The question remains if the Earth's dynamo is indeed highly supercritical. A first estimate of the magnetic Reynolds number, based on a length scale of 2000 km, a velocity scale of 0.5 mm/s, and a magnetic diffusivity of $\lambda := (\mu\sigma)^{-1} \sim 2\,\mathrm{m}^2/\mathrm{s}$ [57], provides $Rm \sim 500$. At least, and apart from all uncertainties, this number does not exclude a highly supercritical state. Hence, whatever the concrete flow field in the Earth might be, it is not a surprise that the resulting dynamo is prone to reversals.

Acknowledgments

This work was supported by Deutsche Forschungsgemeinschaft in frame of SFB 609 and Grant No. GE 682/12-2.

References

[1] F. Stefani, G. Gerbeth, Asymmetric polarity reversals, bimodal field distribution, and coherence resonance in a spherically symmetric mean-field dynamo model, Phys. Rev. Lett. 94 (2005) 184506.
[2] R.T. Merrill, M.W. McElhinny, P.L. McFadden, The Magnetic Field of the Earth, Academic Press, San Diego, CA, 1996.
[3] J.-P. Valet, L. Meynadier, Geomagnetic field intensity and reversals during the past 4 million years, Nature 366 (1993) 234–238.
[4] L. Meynadier, J.-P. Valet, F.C. Bassinot, N.J. Shackleton, Y. Guyodo, Asymmetrical saw-tooth pattern of the geomagnetic field intensity from equatorial sediments in the Pacific and Indian oceans, Earth Planet. Sci. Lett. 126 (1994) 109–127.
[5] S.W. Bogue, H.A. Paul, Distinctive field behavior following geomagnetic reversals, Geophys. Res. Lett. 20 (1993) 2399–2402.
[6] A. Cox, Length of geomagnetic polarity intervals, J. Geophys. Res. 73 (1968) 3247–3259.
[7] J.A. Tarduno, R.D. Cottrell, A.V. Smirnov, High geomagnetic intensity during the mid-Cretaceous from Thellier analysis of single plagioclase crystals, Science 291 (2001) 1779.
[8] M. Fuller, R. Weeks, Geomagnetism—superplumes and superchrons, Nature 356 (1992) 16–17.
[9] R.L. Larson, The midcretacious superplume episode, Sci. Am. 272 (2) (1995) 82–86.
[10] P.R. Vogt, Changes in geomagnetic reversal frequency at times of tectonic change: evidence for coupling between core and upper mantle processes, Earth Planet. Sci. Lett. 25 (1975) 313–321.
[11] R.L. Larson, P. Olson, Mantle plumes control magnetic reversal frequency, Earth Planet. Sci. Lett. 107 (1991) 437–447.
[12] D.E. Loper, On the correlation between mantle plume flux and the frequency of reversals of the geomagnetic field, Geophys. Res. Lett. 19 (1992) 25–28.
[13] D.E. Loper, Mantle plumes and the periodicity of magnetic field reversals, Geophys. Res. Lett. 13 (1986) 1525–1528.
[14] P. Olson, V. Lee Hagee, Geomagnetic polarity reversals, transition field structure, and convection in the outer core, J. Geophys. Res. 95 (1990) 4609–4620.
[15] M. Perrin, V.P. Shcherbakov, Paleointensity of the Earth's magnetic field for the past 400 Ma: evidence for a dipole structure during the mesozoic low, J. Geomagn. Geoelectr. 49 (1997) 601–614.
[16] V.P. Shcherbakov, G.M. Solodovnikov, N.K. Sycheva, Variations in the geomagnetic dipole during the past 400 million years (volcanic rocks), Izvestiya, Phys. Solid Earth 38 (2) (2002) 113–119.
[17] R. Heller, R.T. Merrill, P.L. McFadden, The two states of paleomagnetic field intensities for the past 320 million years, Phys. Earth Planet. Inter. 135 (2003) 211–223.
[18] G.A. Glatzmaier, P.H. Roberts, A 3-dimensional convective dynamo solution with rotating and finitely conducting inner core and mantle, Phys. Earth Planet. Inter. 91 (1995) 63–75.

[19] G.A. Glatzmaier, Geodynamo simulations—how realistic are they? Annu. Rev. Earth Planet. Sci. 30 (2002) 237–257.
[20] P.D. Mininni, D.C. Montgomery, A.G. Pouquet, A numerical study of the alpha model for two-dimensional magnetohydrodynamic turbulent flows, Phys. Rev. E 71 (2005) 046304.
[21] A. Giesecke, U. Ziegler, G. Rüdiger, Geodynamo α-effect derived from box simulations of rotating magnetoconvection, Phys. Earth Planet. Inter. 152 (2005) 90–102.
[22] M. Schrinner, K.-H. Rädler, D. Schmitt, M. Rheinhardt, U. Christensen, Mean-field view on rotating magnetoconvection and a geodynamo model, Astron. Nachr. 326 (2005) 245–249.
[23] T. Rikitake, Oscillations of a system of disk dynamos, Proc. Camb. Philos. Soc. 54 (1958) 89–105.
[24] F. Plunian, P. Marty, A. Alemany, Chaotic behaviour of the Rikitake dynamo with symmetric mechanical friction and azimuthal currents, Proc. R. Soc. London, Ser. A 454 (1995) 1835–1842.
[25] P. Hoyng, M.A.J.H. Ossendrijver, D. Schmitt, The geodynamo as a bistable oscillator, Geophys. Astroph. Fluid Dyn. 94 (2001) 263–314.
[26] D. Schmitt, M.A.J.H. Ossendrijver, P. Hoyng, Magnetic field reversals and secular variation in a bistable geodynamo model, Phys. Earth Planet. Inter. 125 (2001) 119–124.
[27] P. Hoyng, D. Schmitt, M.A.J.H. Ossendrijver, A theoretical analysis of the observed variability of the geomagnetic dipole field, Phys. Earth Planet. Inter. 130 (2002) 143–157.
[28] S. Lorito, D. Schmitt, G. Consolini, P. De Michelis, Stochastic resonance in a bistable geodynamo model, Astron. Nachr. 326 (2005) 227–230.
[29] G. Consolini, P. De Michelis, Stochastic resonance in geomagnetic polarity reversals, Phys. Rev. Lett. 90 (2003) 058501.
[30] T. Yamazaki, H. Oda, Orbital influence on earth's magnetic field: 100,000-year periodicity in inclination, Science 295 (2002) 2435–2438.
[31] A.P. Roberts, M. Winklhofer, W.T. Liang, et al., Testing the hypothesis of orbital (eccentricity) influence on earth's magnetic field, Earth Planet. Sci. Lett. 216 (2003) 187–192.
[32] A. Gailitis, O. Lielausis, E. Platacis, G. Gerbeth, F. Stefani, Colloquium: laboratory experiments on hydromagnetic dynamos, Rev. Mod. Phys. 74 (2002) 973–990.
[33] E.N. Parker, Generation of magnetic fields in astrophysical bodies: IV. Solar and terrestrial dynamos, Astrophys. J. 164 (1971) 491–509.
[34] H. Yoshimura, Z. Wang, F. Wu, Linear astrophysical dynamos in rotating spheres: mode transition between steady and oscillatory dynamos as a function of dynamo strength and anisotropic turbulent diffusivity, Astrophys. J. 283 (1984) 870–878.
[35] G.R. Sarson, C.A. Jones, A convection driven geodynamo reversal model, Phys. Earth Planet. Inter. 111 (1999) 3–20.
[36] W. Deinzer, H.-U.v. Kusserow, M. Stix, Steady and oscillatory α-ω dynamos, Astron. Astrophys. 36 (1974) 69–78.
[37] M.L. Dudley, R.W. James, Time-dependent kinematic dynamos with stationary flows, Proc. R. Soc. London, A 425 (1989) 407–429.
[38] T. Kato, Perturbation Theory of Linear Operators, Springer, Berlin, 1966.
[39] U. Günther, F. Stefani, G. Gerbeth, The MHD α^2-dynamo, $\mathbb{Z}_2$-graded pseudo-Hermiticity, level crossings and exceptional points of branching type, Czech. J. Phys. 54 (2004) 1075–1089.
[40] A.P. Seyranian, O.N. Kirillov, A.A. Mailybaev, Coupling of eigenvalues of complex matrices at diabolic and exceptional points, J. Phys. A 38 (2005) 1723–1740.
[41] U. Günther, F. Stefani, Third order spectral branch points in Krein space related setups: PT-symmetric matrix toy model, MHD α^2-dynamo, and extended Squire equation, Czech. J. Phys. 55 (2005) 1099–1106.
[42] C. Dembowski, B. Dietz, H.D. Graf, H.L. Harney, A. Heine, W. D. Heiss, A. Richter, Experimental observation of the topological structure of exceptional points, Phys. Rev. Lett. 86 (2001) 787–790.
[43] M.V. Berry, The optical singularities of bianisotropic crystals, Proc. R. Soc. A 461 (2005) 2071–2098.
[44] H. Baumgärtel, Analytic perturbation theory for matrices and operators, Akademie-Verlag, Berlin, 1984, and Operator Theory: Adv. Appl. 15, Birkhäuser Verlag, Basel, 1985.
[45] M.V. Berry, M. Wilkinson, Diabolical points in the spectra of triangles, Proc. R. Soc. London, A 392 (1984) 15–43.
[46] A. Brandenburg, F. Krause, R. Meinel, D. Moss, I. Tuominen, The stability of nonlinear dynamos and the limited role of kinematic growth rates, Astron. Astrophys. 213 (1989) 411–422.
[47] R. Meinel, A. Brandenburg, Behaviour of highly supercritical α-effect dynamos, Astron. Astrophys. 238 (1990) 369–376.
[48] A. Gailitis, O. Lielausis, E. Platacis, G. Gerbeth, F. Stefani, Riga dynamo experiment and its theoretical background, Phys. Plasmas 11 (2004) 2838–2843.
[49] A. Gailitis, O. Lielausis, G. Gerbeth, F. Stefani, Dynamo experiments, in: S. Molokov, R. Moreau, H.K. Moffatt (Eds.), Magnetohydrodynamics: Evolution of Ideas and Trends, Springer/Kluwer, Berlin, 2006, to appear.
[50] F. Krause, K.-H. Rädler, Mean-field Magnetohydrodynamics and Dynamo Theory, Akademie-Verlag, Berlin, 1980.
[51] T. Nakajima, M. Kono, Kinematic dynamos associated with large scale fluid motions, Geophys. Astrophys. Fluid Dyn. 60 (1991) 177–209.
[52] F. Stefani, G. Gerbeth, Oscillatory mean-field dynamos with a spherically symmetric, isotropic helical turbulence parameter α, Phys. Rev. E 67 (2003) 027302.
[53] P. Olson, Geomagnetic polarity reversals in a turbulent core, Phys. Earth Planet. Inter. 33 (1983) 260–274.
[54] B. van der Pol, On relaxation oscillations, Philos. Mag. 2 (1926) 978–992.
[55] P. Bak, C. Tang, K. Wiesenfeld, Self-organized criticality, Phys. Rev. A 38 (1988) 364–374.
[56] B.M. Clement, Dependence of the duration of geomagnetic polarity reversals on site latitude, Nature 428 (2004) 637–640.
[57] P.H. Roberts, G.A. Glatzmaier, Geodynamo theory and simulations, Rev. Mod. Phys. 72 (2000) 1081–1123.